Intraparticulate metal speciation analysis of soft complexing nanoparticles : the intrinsic chemical heterogeneity of metal-humic acid complexes

Intraparticulate Metal Speciation Analysis of Soft Complexing Nanoparticles. The Intrinsic Chemical Heterogeneity of Metal-Humic Acid Complexes

Raewyn M. Town[*a,b,c] and Herman P. van Leeuwen[b]

[a] Department of Physics, Chemistry and Pharmacy, University of Southern Denmark, Campusvej 55, 5230 Odense, Denmark. Tlf: +45 65502503, Email: raewyn.town@sdu.dk

[b] Physical Chemistry and Soft Matter, Wageningen University & Research, Stippeneng 4, 6708 WE Wageningen, The Netherlands. Email: herman.vanleeuwen@wur.nl

[c] Systemic Physiological and Ecotoxicological Research (SPHERE), Department of Biology, University of Antwerp, Groenenborgerlaan 171, 2020 Antwerp, Belgium

ABSTRACT

The Counterion Condensation-Donnan (CCD) model for the electrostatic features of soft, charged nanoparticles (NPs) is applied to the determination of the intrinsic stability constants, $\overline{K}_{int}$, for inner-sphere Cd(II) and Cu(II) complexes with humic acid NPs. The novel CCD model accounts for the strong ion condensation potential for higher valency counterions within the intraparticulate double layer zone of the soft NP. The approach offers new insights into the intrinsic heterogeneity of the HA complexes, as revealed by the intraparticulate speciation as a function of the true degree of inner-sphere complexation, θ_M. The ensuing intrinsic heterogeneity parameters, Γ, for CdHA and CuHA complexes are in very good agreement with those obtained from dynamic electrochemical stripping chronopotentiometric measurements. The overall intraparticulate metal ion speciation is found to depend on θ_M: at low θ_M the strong inner-sphere complexes predominate whilst at higher θ_M values, electrically condensed M may be an equally significant or even larger fraction of the particle-associated M.

INTRODUCTION

Humic acids (HA) are soft charged nanoparticles (NPs) that play an important role in buffering concentrations of metal ions in environmental media.[1-3] They are chemically and physically heterogeneous. Accordingly, their physicochemical properties such as size and chemical functionality cannot be described by singular characteristic parameters. For example, the stability of metal complexes with HA is described by a distribution that characterises the affinity as a function of the degree of binding site occupation.[1] At near neutral pH, HAs carry a substantial net negative charge.[2,4] The ensuing particle electric field influences the extent to which oppositely charged ions associate with the HA entities as well as the chemodynamic features of the complexes formed.[5] Accordingly, the soft and permeable intraparticulate environment contains partitioning free metal ions as well as electrostatically associated metal ions, in addition to metal ions bound in inner-sphere complexes with HA binding sites.[6] The extent of electrostatic interaction is predominantly governed by the net charge on the metal ion, whilst inner-sphere complex formation is governed by the chemical affinity between the target metal ion, M, and the pertaining binding sites, S. As a consequence, the HA complexes of e.g. Cu(II) are known to be significantly stronger and more heterogeneous than those of Cd(II).[1,7] A rigorous understanding of the equilibrium and dynamic features of nanoparticulate metal complexes evidently calls for *intraparticulate* speciation analysis.

We have recently shown that the electrostatic contribution to cation binding by charged soft particles can be described by a counterion condensation-Donnan model (CCD).[6,8,9] Development of the CCD approach arose from the observation that the extent to which the predominantly electrostatically binding Ca^{2+} associates with HA is massively underestimated by continuous Poisson-Boltzmann electrostatics.[8] The interactions of Ca^{2+} with HA at high negative charge density are predominantly electrostatic with covalent contributions being insignificant.[10,11] It was found that the extent to which aqueous Ca^{2+} ions associate with several types of HA at different ionic strengths can be well described by the CCD model which combines (i) electric condensation of counterions in the strongly charged intraparticulate double layer (DL) shell at the particle/medium interface with (ii) Donnan partitioning in the net uncharged core of the particle body.[6] Strong condensation is found for 2+ ions in the DL zone of HA. Indeed, the

condensation limit found for 2+ ions corresponds to a local concentration within the DL shell on the order of several hundred mol m^{-3}, in line with findings for polyelectrolytes such as DNA.[12] Furthermore, the extent of condensation is in convincing agreement with the charge/potential characteristics of the double layer at the particle/medium interface.[6] Others have shown that Ca^{2+} and Ba^{2+} exhibit condensation behavior with HA.[13] Indeed, counterion condensation is a general phenomenon applicable to polyions of any geometry with sufficient charge density, e.g. it has been invoked to describe the extent of ion binding by DNA,[12] dendrimers,[14-16] and core-shell nanoparticles with a 3D structural charge in the shell.[17] The CCD model provides a physicochemically consistent description of the intraparticulate speciation of various metal ions associated with sufficiently large HA particles, including cases which also involve inner-sphere complex formation. [6,8,9] To date the CCD approach has been used to determine intrinsic stability constants, $\overline{K}_{\mathrm{int}}$, for Cd(II), Pb(II) and Cu(II) complexes with HA at a single degree of inner-sphere complexation, θ_{M}.[6] The magnitude of θ_{M} corresponds to the ratio of the intraparticulate concentrations of inner-sphere complexes, MS, and total reactive sites, S, i.e. $c_{\mathrm{MS}} / c_{\mathrm{S,t}}$. The over-bar notation for $\overline{K}_{\mathrm{int}}$ signifies that the intrinsic stability represents a weighted average of all the inner-sphere complexes that are formed at the applicable θ_{M}. The agreement between $\overline{K}_{\mathrm{int}}$ values derived from CCD analysis of measurements in KNO_3 and $Ca(NO_3)_2$ electrolyte established the consistency of the model in its accounting for electrostatic contributions to metal binding.[9] Here we aim to broaden the scope and apply the CCD analysis of the intraparticulate speciation to the determination of $\overline{K}_{\mathrm{int}}$ values for CdHA and CuHA as a function of θ_{M}. The ensuing intrinsic heterogeneity parameters will be compared with established descriptors of the heterogeneity of HA complexes.

THEORY

Experimental determinations of metal ion binding by soft charged NPs involve measurement of the concentrations of 'bound' and 'free' metal ions, e.g. by ion selective electrode potentiometry in the medium phase. The corresponding apparent stability constants, $\overline{K}_{\mathrm{app}}$, contain both electrostatic and chemical affinity contributions to the binding. That is, the 'bound' M collectively includes all forms of M

that are associated with the NP, including the *free* M within the particle body and in the interfacial double layer. It follows that $\overline{K}_{app}$ values have limited meaning for understanding the true nature of the inner-sphere metal-HA site complex within the particle body, where the prevailing conditions, e.g. pH, ionic strength and ensuing effective charge screening can differ substantially from those in the surrounding bulk solution. Conversion of $\overline{K}_{app}$ values for different metal-to-binding site ratios to intrinsic chemical stability constants, $\overline{K}_{int}$, therefore requires careful accounting for the electrostatic contributions to metal ion binding, as we shall discuss in detail below. We shall consider the situation where a highly charged soft NP is equilibrated in an aqueous solution of a non-complexing background electrolyte which has a concentration well in excess over the smeared-out concentration of NP charged sites.

Intrinsic stability constants

The intrinsic stability constant $\overline{K}_{int}$ describes the inherent chemical affinity between M and S; it does not include the effects of cooperative multicharge electrostatics beyond the atom-atom scale. Most of the literature on ion binding by HA is based on the assumption that electrostatic association of counterions with the HA particle entity is involved with Donnan-type partitioning only.[18-22] For the case of highly charged soft particles, with (i) a radius, r_p, well above the intraparticulate screening length, κ_p^{-1},[23] and (ii) an average structural charge separation, ℓ_C, sufficiently small so that $\kappa_p \ell_C$ is well below unity, a Donnan potential difference, ψ_D, is established between the bulk of the soft particle phase and the bulk aqueous medium:

$$\psi_D = \frac{RT}{zF} \operatorname{asinh}\left(\frac{\rho_p}{2zFc_1} \right) \qquad (1)$$

where $z_- = z_+ = z$ is the valence of the symmetrical excess background electrolyte with bulk concentration c_1, ρ_p is the structural volume charge density due to charged groups on the backbone of the soft body, and other constants have their usual meaning. For small particles that do not satisfy the $\kappa_p r_p >> 1$ criterion, the non-linear Poisson-Boltzmann approach can be used to compute the extent to which ions are electrostatically accumulated by the particle body.[24,25] Expressions are also available to compute ψ_D for

asymmetrical electrolytes.[26] The magnitude of ψ_D governs the extent to which ions of type i, with valency z_i, partition between the soft particle phase (where its concentration is $c_{i,D}$) and the electrolyte solution (where its concentration is c_i^*) according to the average Boltzmann factor, $\overline{f}_B$, over the applicable spatial zone:[27]

$$\overline{f}_{B,i} = \frac{c_{i,D}}{c_i^*} = \exp\left(\frac{-z_i F \psi_D}{RT}\right) \quad (2)$$

For the present case of a large excess of non-complexing background electrolyte over the target metal ion, ψ_D is governed by the background electrolyte. Minor counterions then accumulate according to a Boltzmann factor $\exp(-\psi_D)$, eq 2, and in its simplest form the ensuing correction for the relationship between $\overline{K}_{app}$ and $\overline{K}_{int}$ is:

$$\overline{K}_{int} = \overline{K}_{app} / \overline{f}_{B,M} \quad (3)$$

However, even when the electrostatic contribution to $\overline{K}_{app}$ involves only Donnan-type partitioning, the translation to a $\overline{K}_{int}$ value should also involve accounting for the differences in physicochemical conditions between the aqueous medium and the particle body, e.g. the effective ionic strength and charge screening, the available outer-sphere volume, *etc*., as well as the presence of intraparticulate species of M other than the inner-sphere complexes. Comparison of data obtained in different types of background electrolyte, e.g. 1:1 versus 2:1, can give insights into the physicochemical consistency of the electrostatic corrections employed in the derivation of $\overline{K}_{int}$.

For the general case of very strong positional correlations between highly charged particles and their counterions, Poisson-Boltzmann theory loses its applicability.[28] In line with this, recent work has shown that mere Donnan partitioning significantly underestimates the extent to which the predominantly electrostatically binding Ca^{2+} ion associates with HA.[6,8] This observation led to the development of the two-state Counterion Condensation-Donnan model. That is, the Ca^{2+}-HA association can be described solely in terms of electrostatics by combining counterion condensation[12,29] in the intraparticulate double layer with Donnan partitioning in the remainder of the particle body. Specifically, the CCD approach

divides the volume of an individual soft particle into two zones: (i) a strongly charged intraparticulate double layer zone (thickness ℓ_{DL}, volume V_{DL}, volume fraction φ_{DL}, condensation limit for 2+ counterions $\overline{f}_C$) in which electric condensation of target metal ions M^{2+} takes place, and (ii) the remaining bulk interior of the NP body (volume V_D, volume fraction φ_D) which behaves as a true Donnan phase with no net charge and a constant potential throughout.[6,8] A potential drop of *ca*. -70 mV over the intraparticulate double layer[4] corresponds to an uncompensated charge density of -140 mol *e* m^{-3} (20% of the structural charge for the present HA) within an ℓ_{DL} of 2 nm which yields a shell charge of -0.025 C per m^2 surface area.[6] The assumption of a constant ψ_D within V_D requires $\kappa_p r_p >> 1$, i.e. a volume fraction ratio φ_{DL}/φ_D much less than unity. For the HA entities considered herein φ_{DL}/φ_D is less than 0.1. With the differentiated CCD electrostatic model for soft charged NPs, the intrinsic stability constant is defined in terms of the applicable intraparticulate conditions and reactant concentrations. For the present high charge density case, the $\overline{K}_{int}$ within V_D is thus given by:

$$\overline{K}_{int} = \frac{c_{MS}^{D}}{c_{M,f}^{D} c_{S}^{D}} \qquad (4a)$$

where c_{MS}^{D}, $c_{M,f}^{D}$ and c_{S}^{D} are the local *intraparticulate* average concentrations of inner-sphere complexes, free metal ions and reactive sites in V_D, respectively. In the high charge density regime the outer-sphere volume around a complexing site and the remaining aqueous volume of the particle are at practically the same potential.[30] In such a case the intraparticulate free metal ion and the outer-sphere associates are electrostatically nearly equivalent and interconversion between these species is very fast. Accordingly, most of the ion pairing energy is accounted for in the energy change that occurs when M enters the particle, i.e. $\overline{f}_{B,M}$. In a similar vein, within the double layer zone of a highly charged particle the condensed ions and the free M will have comparable energy levels. In such case the condensed M^{2+}, M_{cond}, will thus count explicitly in $\overline{K}_{int}$, i.e.:

$$\overline{K}_{int} = \frac{c_{MS}^{DL}}{(c_{M,f}^{DL} + c_{M,cond}^{DL}) c_{S}^{DL}} \qquad (4b)$$

where the superscript DL denotes the average concentrations of the various M species in the DL. For particles with lower charge density, in which there is a finite and significant energy difference between the condensed and free M, the $c_{\mathrm{M,cond}}^{\mathrm{DL}}$ in eq 4b will carry a coefficient greater than unity since the condensed ions will have the lower energy level. On passing from high to low charge density domains, the cooperative electrostatics of condensation gradually evolve into individual ion pair behaviour, as e.g. applicable in the well-known Eigen mechanism for aqueous complex formation reactions. Within the DL zone the metal speciation will be a function of position due to the potential gradient and the ensuing gradient in the concentration of free M. Generally, within the DL of a highly charged NP complexant, the sum of $c_{\mathrm{M,cond}}^{\mathrm{DL}}$ and $c_{\mathrm{MS}}^{\mathrm{DL}}$ will be much greater than $c_{\mathrm{M,f}}^{\mathrm{DL}}$. The ensuing intraparticulate metal ion speciation scheme for high charge density soft NP complexants has been published previously,[6] and the procedure is described in the Experimental section below.

Heterogeneity of metal complexation by HA

The CCD-derived $\overline{K}_{\mathrm{int}}$ values, eq 4, allow us to explore the intrinsic chemical heterogeneity features of multi-site complexants such as HA. At a given metal-to-binding site ratio, the metal ion will form complexes with a certain fraction of the available HA binding sites. There is a significant body of literature on the heterogeneity of MHA complexes, and it is generally found that the degree of heterogeneity follows the order Cd(II) < Pb(II) < Cu(II).[1,7] It has been demonstrated for HA that a double logarithmic plot of K versus θ_{M} comes to a straight line with slope equal to $-1/\Gamma$, where Γ is the heterogeneity parameter ($0 < \Gamma \leq 1$; $\Gamma = 1$ for the homogeneous case).[1,31] Such a relationship has been demonstrated to also apply to apparent-type stability constants and makes no *a priori* assumption about the nature of the metal binding isotherm. The relationship:

$$\log\theta_{\mathrm{M}} = \text{constant} - \Gamma \log K \qquad (5)$$

has the form of a Freundlich isotherm.[32] The Freundlich type distribution has been applied to interpretation of the association/dissociation kinetics of MHA complexes,[33] and to description of the shape of voltammetric[31] and stripping chronopotentiometric waves.[7]

EXPERIMENTAL / COMPUTATION

Reagents and solution conditions

Solutions were buffered to pH 6 with 1 mol m^{-3} MES buffer ((2-(*N*-morpholino)-ethanesulfonic acid) prepared from the solid (Fluka, MicroSelect, ≥ 99.5%): MES buffer has a low affinity for Cd(II) and Cu(II).[34,35] Ionic strength was maintained at 10 mol m^{-3} or 100 mol m^{-3} with KNO_3 or $Ca(NO_3)_2$ (BDH, AnalaR). M(II) solutions were prepared by dilution of standards (Aldrich). All solutions were prepared in ultrapure deionized water (resistivity > 18 MΩ cm) from a Milli-Q gradient system.

The HA sample was from Aldrich and dynamic light scattering measurements indicate that the particles have an approximately constant particle radius, r_p, of *ca*. 80 nm over the pH range 5 to 8 and ionic strength range 0 to 400 mol m^{-3} KCl.[36,37] The total carboxyl group content of Aldrich HA is *ca*. 3 mol per kg of HA.[38,39] Accordingly, the effective charge density within the particle is *ca*. -700 mol m^{-3} in an electrolyte medium at pH 6 (determined using the HA density of 1.66 kg m^{-3} and an 80% water content).[40] Within the particle body the pH will be at least 1 unit below that in the bulk medium, and thus carboxylate groups will be the predominant structural charge carriers and reactive sites under our experimental conditions. The CCD analysis makes no *a priori* assumption about the nature of the sites, e.g. carboxylic or phenolic type, that give rise to the charge density and/or are involved in metal ion complexation. In all experiments in this work the concentration of HA in the dispersion was 25 to 50 g m^{-3}, corresponding to a volume fraction on the order of 10^{-4}.

Electrochemical measurements

The concentration of free M_{aq}^{2+} in the bulk medium, $c_{M,f}^{*}$, was determined by stripping chronopotentiometry at scanned deposition potential (SSCP)[41] and Absence of Gradients and Nernstian Equilibrium Stripping (AGNES).[42] The heterogeneity parameter, Γ, was determined from the shape of the SSCP waves as described previously.[7] SSCP allows the effect of heterogeneity in the metal complexation to be unambiguously distinguished from e.g. any (change in the) degree of electrochemical reversibility.[43,44] For both Cd(II) and Cu(II), the metal-only systems were electrochemically reversible

under the given conditions, as evidenced from the log analysis of the SSCP waves, i.e. slope of *ca*. 30 mV in both cases.[45,46] In the presence of HA, the slope of the SSCP waves for both Cd(II) and Cu(II) was decreased relative to the metal-only cases, and was independent of the deposition time. If any degree of electrochemical reversibility would be present, then the impact of this on the SSCP slope would be mitigated at longer deposition times.[45] Accordingly, the change in the slope of the SSCP wave upon addition of HA can be unambiguously ascribed to heterogeneity in the metal speciation.[43-45] Electrochemical measurements were performed with an Ecochemie μAutolab potentiostat coupled with a Metrohm 663 VA stand. The oxidation step was performed under complete depletion conditions (stripping current = 2 nA).[47] The electrometer input impedance of these instruments is > 100 GΩ. The working electrode was a Metrohm multimode mercury drop electrode, the auxiliary electrode was glassy carbon, and the reference electrode was Ag|AgCl|KCl(sat) encased in a 100 mol m^{-3} KNO_3 jacket. Solutions were initially purged with oxygen-free N_2, and a nitrogen blanket was maintained during measurements.

Intraparticulate speciation computation

The volume fraction of HA in the dispersion was used to convert smeared-out concentrations into local intraparticulate ones. At sufficiently high θ_M values, the total M associated with the particle is greater than that required to satisfy the electrostatic demands, i.e. the accumulation of M^{2+} according to the pertaining $\overline{f}_{B,M}$ in V_D and V_{DL}, eq 2, and the condensation of M^{2+} to compensate for the prescribed fraction of the charge in the intraparticulate DL (see ref 6 for details). In brief, the electrostatic parameters for the CCD model are established from the extent to which the aqueous Ca^{2+} ion associates with several types of HA particles. A consistent description of the Ca^{2+}-HA association data was obtained for 80% charge compensation the intraparticulate double layer of thickness, ℓ_{DL}, of 2 nm together with Donnan partitioning in the remainder of the particle body. For the present HA, an uncompensated charge of -140 mol m^{-3} (20% of the structural charge) within an ℓ_{DL} of 2 nm in a particle of radius 80 nm corresponds to a surface charge, σ_s of -0.025 C m^{-2}. The corresponding potential drop over the intraparticulate DL ($=\sigma_s \ell_{DL} / \varepsilon\varepsilon_0$) of *ca*. -70 mV is of the correct order of magnitude, certainly if it is

taken into account that the density of deprotonated carboxyl groups is slightly higher in the more hydrophilic outer regions of the HA particle body.[48] For the association of M, which also includes convalent contributions to the binding, the intraparticulate speciation is computed by satisfying the electrostatic demands and ascribing the remaining M to inner-sphere complexes. The total concentration of M within the particle body, $c_{M,t}$, is given by:

$$c_{M,t} = c_{M,f}^{D}\varphi_{D} + (c_{M,f}^{DL} + c_{M,cond}^{DL})\varphi_{DL} + c_{MS} \quad (6)$$

where $c_{M,f}^{D}$ is given by $\overline{f}_{B,M}c_{M,f}^{*}$ and c_{MS} is the average concentration of MS in the entire particle volume. For the present purposes of characterising the heterogeneity of a nanoparticulate HA complexant, we make the assumption that the average c_{MS} in V_{DL} is approximately the same as that in V_{D}. According to chemical equilibrium conditions in the DL zone, eq 4b, the concentration of MS should follow the gradient in the concentration of free M. Thus, since $\varphi_{DL}/\varphi_{D} << 1$, the contribution of c_{MS}^{DL} to c_{MS} is small. Similarly, the average concentration of free M in the DL represents an insignificant proportion of the total intraparticulate M: $c_{M,f}^{DL}$ was estimated by taking the potential at the particle/medium interface to be *ca*. 2/3 of the Donnan potential.[6,49,50] The presence of MS in the DL reduces the net charge therein, and thus the condensation demand is correspondingly decreased. Accordingly, the initial intraparticulate metal speciation is iterated with respect to the concentration of inner-sphere complexes in the entire particle body versus that of the condensed metal ions in the DL zone until a consistent distribution of the different species over both the Donnan bulk and the DL zone is attained that satisfies the overall charge compensation (see Theory). Consistent values for c_{MS} and $c_{M,cond}^{DL}$ were attained after *ca*. 4 iterations in all cases. In $Ca(NO_3)_2$ background electrolyte the condensation requirements are met by Ca^{2+},[9] thus the electrostatic demands for M^{2+} reduce to the simple Boltzmann accumulation according to the applicable $\overline{f}_{B,M}$ for the 2:1 electrolyte in both V_{D} and V_{DL}. The presence of MS in V_{D} reduces the net charge therein, but for the θ_{M} range considered this effect has negligible impact on the applicable $\overline{f}_{B,M}$ values. For example, at the highest θ_{M} considered, and an ionic strength of 10 mol m^{-3}, the reduction in $\overline{f}_{B,M}$ due to the presence of MS translates to a difference of 0.2 in the computed log $\overline{K}_{int}$. The agreement between the $\overline{K}_{int}$ values obtained from measurements in KNO_3 and $Ca(NO_3)_2$ electrolyte confirm the consistency of

the approach and the electrostatic parameters employed (see Results and Discussion).[9] Below a certain θ_M value, the total M associated with the particle is less than that required to satisfy the electrostatic demands in KNO_3 electrolyte and bulk medium becomes strongly depleted. In such cases the $\overline{K}_{int}$ computed from measurements in $Ca(NO_3)_2$ provides the starting point to compute the concentration of inner-sphere complexes, which are complemented with an appropriate amount of M_{cond} to achieve mass balance, eq 6, then iterated as above.

RESULTS AND DISCUSSION

Here we aim to find the physicochemically most reasonable analysis of the heterogeneity of MHA complex stabilities. The CCD model offers a unique advantage over conventional approaches because it accounts for the conditions prevailing with the particle body. The degree of intrinsic chemical heterogeneity of the complexes is reflected in the extent to which $\overline{K}_{int}$ depends on θ_M. We highlight that the true θ_M corresponds to the concentration ratio of *inner-sphere* bound M, c_{MS}, and total binding sites S, $c_{S,t}$. Accordingly, determination of the intraparticulate distribution of M over the free, condensed, and inner-sphere bound forms is fundamental to establishing the proper θ_M value. The comparison of results obtained in KNO_3 and $Ca(NO_3)_2$ electrolyte provides a means to verify the consistency of the application of the CCD model to obtain $\overline{K}_{int}$ values. The agreement obtained between the $\overline{K}_{int}$ computed from experimental measurements in $Ca(NO_3)_2$ and the $\overline{K}_{int}$ derived from an iterative analysis of the data obtained in KNO_3 (see Experimental) illustrates the inherent consistency of the CCD model and the applicability of the parameters for the HA studied herein (φ_{DL}, ψ_D, $\overline{f}_C$).[9]

Extent of metal binding as a function of θ_M

As the ratio of the total concentrations of M and S in the dispersion is increased, a greater amount of M becomes associated with the HA particles. The intraparticulate speciation of M^{2+} arises from the interplay between the applicable $\overline{K}_{int}$ and the electrostatic demands for the metal ion. Accordingly, the distribution of the total intraparticulate M over its free, condensed and inner-sphere complexed forms is expected to

vary with θ_M. For both Cd(II) and Cu(II), the free ions are generally a minor proportion of the total intraparticulate M over the entire range considered. At the highest θ_M considered (*ca*. 0.1), for both Cd(II) and Cu(II), the amount of M associated with the HA particles is much greater than that required to meet the electrostatic demands. Accordingly, the majority of the intraparticulate M is in the form of inner-sphere complexes. For Cu(II), the overall concentration ratio between condensed ions and inner-sphere complexes, $R_{M_{cond}/MS}$, is *ca*. 0.2 at I = 10 and 100 mol m^{-3}, whilst within the DL zone $R_{M_{cond}/MS}$ is *ca.* 3. Formation of the weaker Cd(II) complexes is more sensitive to ionic strength, implying a significant electrostatic contribution to the binding, with the overall $R_{M_{cond}/MS}$ being *ca*. 0.4 at I = 10 mol m^{-3} and 0.7 at I = 100 mol m^{-3}, and $R_{M_{cond}/MS}$ within the DL zone being *ca*. 6 and 10, respectively. For both Cd(II) and Cu(II), as θ_M decreases the $\overline{K}_{int}$ increases. From the point of view of charge compensation in the DL zone, the inner-sphere complexes are equivalent to the electrostatically condensed ions. Accordingly, the intraparticulate speciation arises from the interplay between the magnitude of $\overline{K}_{int}$ and the total M available to meet the electrostatic and chemical affinity demands of the reactive sites. A lower θ_M corresponds to a lower total concentration of M associated with the particles. For the HA in this study, the outcome is that the overall $R_{M_{cond}/MS}$ decreases as θ_M decreases from *ca*. 0.1 to 0.03. At a θ_M of *ca*. 0.03, the overall $R_{M_{cond}/MS}$ is 1.0 for Cu(II) at both ionic strengths, whilst for Cd(II) the ratio is 1.4 and 2.3 at I = 10 and 100 mol m^{-3}, respectively. As θ_M is decreased further, the chemical affinity increases, with approximately all of the M being in the form of inner-sphere complexes at θ_M *ca*. 0.003, I = 10 mol m^{-3}. The intraparticulate speciation for CdHA and CuHA is summarized in Figure 1 for an ionic strength of 10 mol m^{-3} (KNO_3 electrolyte).

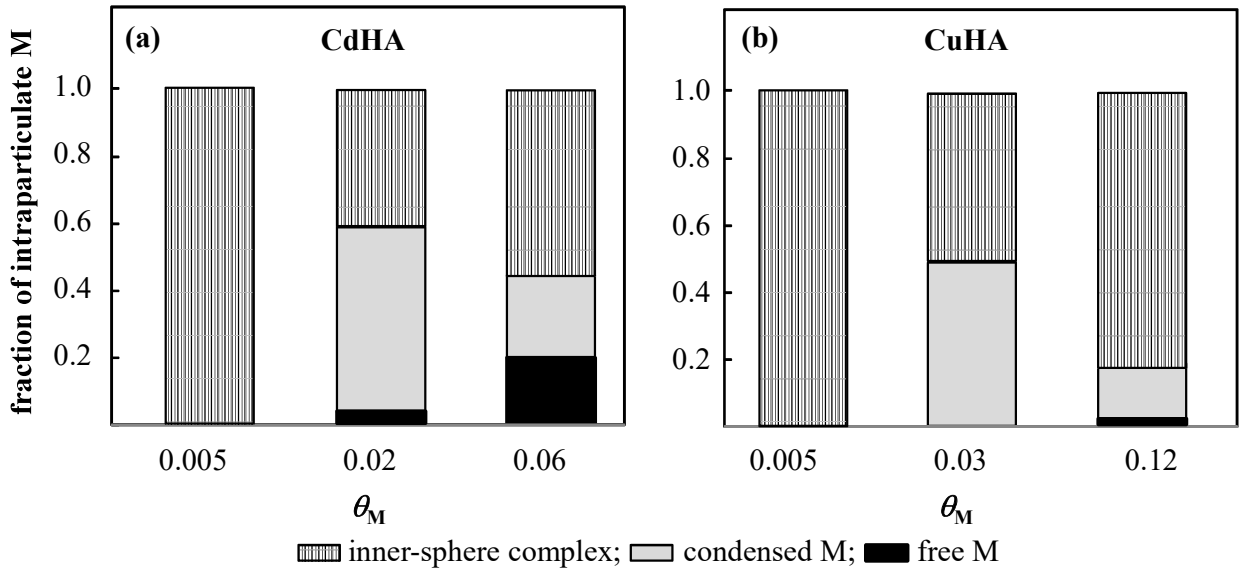

Figure 1. Intraparticulate speciation of (a) Cd(II) and (b) Cu(II) in an aqueous dispersion of HA particles for various values of the true intraparticulate θ_M, i.e. $c_{MS} / c_{S,t}$, as derived from application of the CCD model. The proportions of the different metal species are given in black for the free metal ion, in red for the condensed ions, and in blue for the inner-sphere metal complex species. The bulk medium comprises 10 mol m^{-3} KNO_3 electrolyte at pH 6.

Intrinsic chemical affinity as a function of θ_M

The heterogeneities of the CdHA and CuHA complexes are determined from the evolving slope of the SSCP waves as well as by evaluating the magnitude of the CCD-derived $\overline{K}_{int}$ values as a function of the true θ_M. SSCP effectively scans a range of metal-to-ligand ratios from the foot to the plateau of the wave.[7] This means that the heterogeneity parameter, Γ, can be determined from a single SSCP wave recorded at a given composition of the bulk dispersion. Figure 2 compares the experimental SSCP data with curves computed assuming that the binding follows a Freundlich type distribution. The slope of the SSCP wave changes moderately over the Γ range 0.8 to 0.6, i.e. for metal complex systems such as CdHA that exhibit fairly weak complexation and modest degrees of heterogeneity. Figure 2a shows that the SSCP waves recorded for CdHA are well described by curves computed for Γ values in this range. In contrast, very heterogeneous systems exhibit much greater changes in the slope of the SSCP wave. In line

with this, Figure 2b shows that the SSCP wave recorded for CuHA corresponds to a curve computed for $\Gamma = 0.2$. SSCP waves recorded in KNO_3 and $Ca(NO_3)_2$ electrolyte yielded similar Γ values.

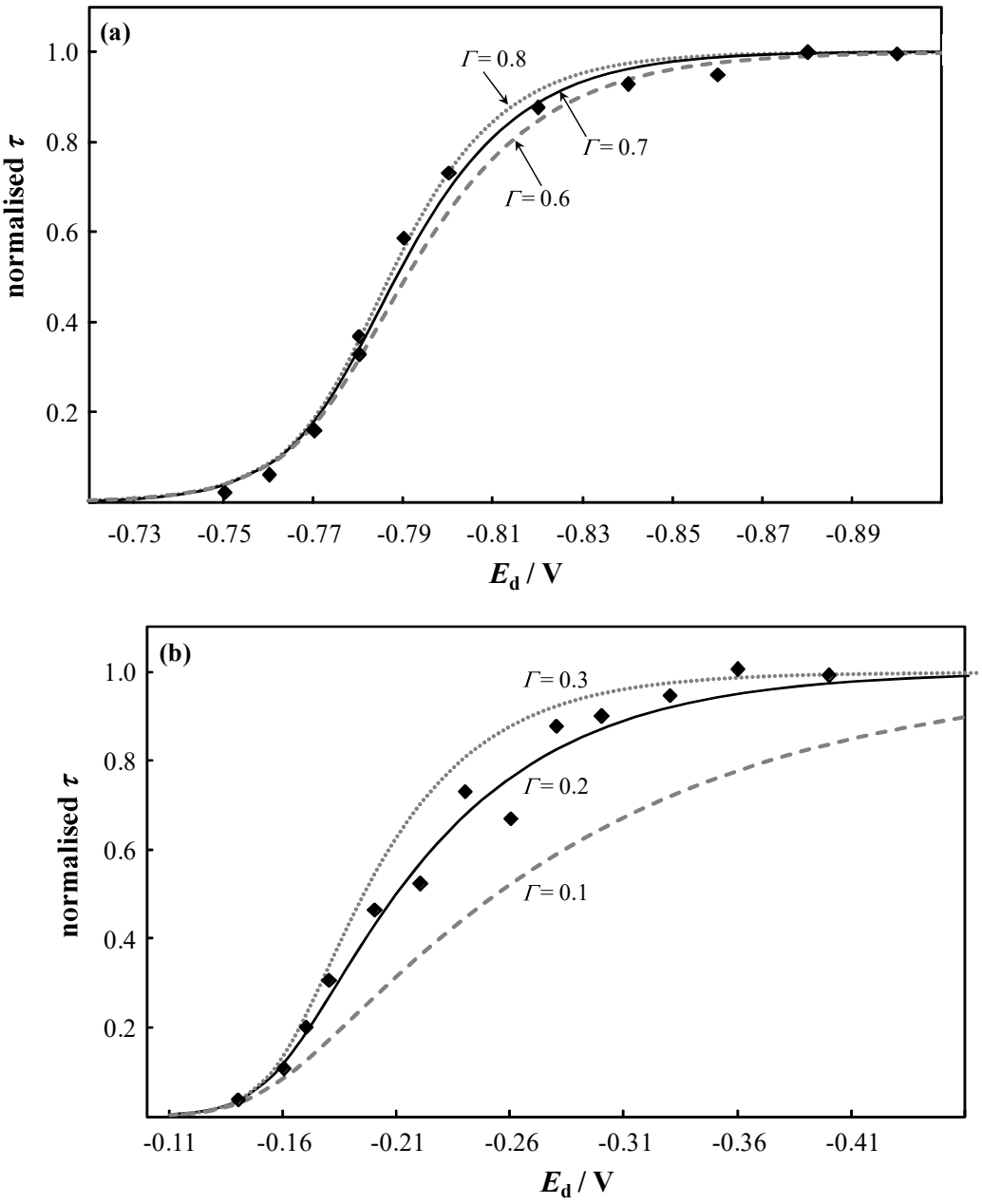

Figure 2. Experimental and computed SSCP waves (normalised reoxidation time, τ, as a function of deposition potential, E_d) for (a) CdHA and (b) CuHA. The experimental data are shown by solid diamonds and the theoretically predicted waves for the indicated Γ values are represented by curves. The experimental data correspond to $\theta_M \approx 0.03$ and were measured in $Ca(NO_3)_2$ electrolyte at pH 6 and ionic strength of 10 mol m^{-3} for CdHA and 100 mol m^{-3} for CuHA.

$\overline{K}_{int}$ values were determined from experimental measurements in both KNO_3 and $Ca(NO_3)_2$ electrolytes at ionic strengths of 10 and 100 mol m^{-3}, using the CCD approach to account for electrostatic contributions to the binding. The intraparticulate environment will be different in KNO_3 as compared to $Ca(NO_3)_2$ electrolyte, in terms of the net charge density and the corresponding ψ_D, the ensuing magnitude of $\overline{f}_{B,M}$ and the effective charge screening. Thus, the attainment of consistent $\overline{K}_{int}$ and Γ values from measurements as a function of θ_M in these two electrolytes is a good test of the robustness of the CCD electrostatic model. From the slope of the double logarithmic plot of $\overline{K}_{int}$ versus θ_M for the CCD-derived data (Figure 3), we obtain a Γ value of *ca*. 0.6 for Cd(II) and *ca.* 0.2 for Cu(II). These CCD-derived Γ values are in really convincing agreement with those derived from the profile of the SSCP waves (Figure 2). These results represent the first physicochemically sound assessment of the intrinsic chemical heterogeneity of metal-HA complexation. If electric condensation of the target M in KNO_3 electrolyte would *not* be taken into account, then the ensuing $\overline{K}_{int}$ and Γ values would not be consistent with those obtained from measurements in $Ca(NO_3)_2$ electrolyte (see red symbols in Figure 3). This outcome thus provides further support for the occurrence of condensation of the target M^{2+}.

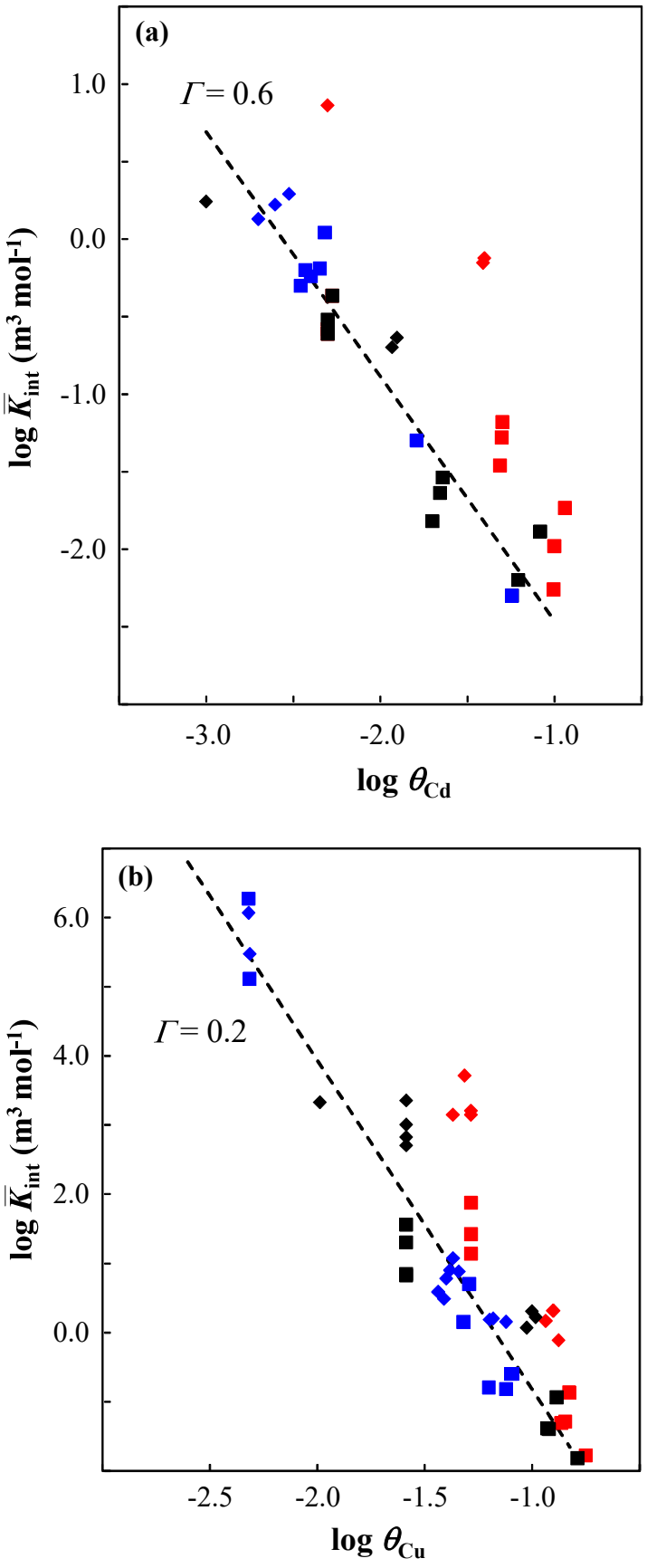

Figure 3. Intrinsic stability constant values, log $\overline{K}_{int}$, as a function of the degree of inner-sphere complexation, log θ_M, for (a) Cd(II) and (b) Cu(II) complexes with HA. The data were obtained from

measurements in KNO_3 electrolyte at I = 10 mol m^{-3} (solid black squares) and 100 mol m^{-3} (solid black diamonds) and in $Ca(NO_3)_2$ electrolyte at I = 10 mol m^{-3} (solid blue squares) and 100 mol m^{-3} (solid blue diamonds). The $\overline{K}_{int}$ values derived from measurements in KNO_3 electrolyte with the assumption that Donnan-partitioning is the only electrostatic contribution to the binding, i.e. neglecting condensation of the target metal ion, are indicated by solid red squares (I = 10 mol m^{-3}) and solid red diamonds (I = 100 mol m^{-3}). The dashed black line, with a slope of -Γ, corresponds to the best fit through all the CCD-derived points, i.e. all the black and blue symbols.

CONCLUSIONS AND OUTLOOK

We highlight that we seek to find the most straightforward, physicochemically consistent description of the intrinsic heterogeneity of metal ion binding by soft, charged HA particles. The work presented herein therefore first of all focusses on the intraparticulate speciation of the target metal ion, which has not been rigorously considered by conventional analysis and modelling tools. It is shown that the electric condensation of the target metal ion in the intraparticulate zone of the double layer at the particle/medium interface may be of substantial proportions and play an essential role in the computation of the true K_{int} of the metal humic acid complex. In line with this, the Counterion Condensation-Donnan model accounts well for the electrostatic contribution to the binding of Cd(II) and Cu(II) by HA. It makes no *a priori* assumptions about the nature of the charged or reactive sites, nor about the metal binding isotherm. For both the moderately heterogeneous CdHA complexes and the very heterogeneous CuHA ones, specific support for the CCD model is provided by (i) the coincidence of the log $\overline{K}_{int}$ versus log θ_M plots for data derived from measurements in both KNO_3 and $Ca(NO_3)_2$ electrolytes at ionic strengths of 10 and 100 mol m^{-3}, and (ii) the agreement between the values of the heterogeneity parameter, Γ, obtained from the slope of the log $\overline{K}_{int}$ versus log θ_M plots and those determined from dynamic electrochemical SSCP data.

The distribution of the particle-associated M over its various intraparticulate forms is found to be dependent on the degree of inner-sphere complexation, θ_M. Thus, the analysis of the intraparticulate metal speciation is fundamental to rigorous interpretation of the true equilibrium features of MHA

systems as well as for predicting their dynamic properties such as chemical reactivity and bioavailability. At low θ_M values, the strongest binding sites govern complexation and inner-sphere complexes are the predominant intraparticulate metal species; as θ_M increases, progressively weaker HA binding sites govern the extent of complexation. Accordingly, at higher θ_M, distinction is progressively lost between strong electric condensation, in which M may exchange some of its inner-sphere water of hydration,[51,52] and weak chemical complexation, in which M may retain some of its primary hydration shell. Work is in progress to quantify the nature of the equilibration between electrically condensed ions, as governed by electrostatic demands, and inner-sphere bound M, as governed by chemical affinities between the metal and the complexing humic acid sites.

Symbols and abbreviations

CC	counterion condensation
D	Donnan phase
DL	double layer
HA	humic acid
I	ionic strength
M	metal ion
S	reactive site
NP	nanoparticle
SSCP	stripping chronopotentiometry at scanned deposition potential
$c^{*}_{M,f}$	concentration of free metal ion in the bulk electrolyte solution (mol m^{-3})
$c^{DL}_{M,f}$	local average concentration of free metal ion in the intraparticulate DL (mol m^{-3})
$c^{D}_{M,f}$	local average concentration of free metal ion in the Donnan volume (mol m^{-3})
$c^{DL}_{M,cond}$	local average concentration of condensed metal ion in the intraparticulate DL (mol m^{-3})

c_{MS}^{DL}	local average concentration of inner-sphere complexes in the intraparticulate DL (mol m^{-3})
c_{MS}^{D}	local average concentration of inner-sphere complexes in the Donnan volume (mol m^{-3})
$c_{M,t}$	local total concentration of all forms of M in the particle body (mol m^{-3})
c_{MS}	local average concentration of inner-sphere complexes within the particle volume (mol m^{-3})
$c_{S,t}$	local total concentration of reactive sites within the particle volume (mol m^{-3})
e	elementary charge
$\overline{f}_{B.M}$	average Donnan partitioning factor for the metal ion
$\overline{f}_{C}$	condensation limit for 2+ ions in the intraparticulate double layer
Γ	heterogeneity parameter
$\overline{K}_{app}$	apparent average stability constant for MHA based on smeared-out concentrations (m^3 mol^{-1})
$\overline{K}_{int}$	intrinsic average stability constant for inner-sphere MS (m^3 mol^{-1})
κ_p^{-1}	intraparticulate Debye length (m)
ℓ_{DL}	thickness of the intraparticulate condensation zone (m)
ℓ_{C}	separation distance between charged sites (m)
r_p	particle radius (m)
$R_{M_{cond}/MS}$	concentration ratio between condensed ions and inner-sphere complexes
V_D	volume of the Donnan phase (m^3)
V_{DL}	volume of the intraparticulate double layer zone (m^3)
ψ_D	Donnan potential (V)
ρ_p	structural volume charge density in the particle body (mol *e* m^{-3})

φ_{DL}	particle volume fraction of the double layer zone
φ_{D}	particle volume fraction of the Donnan zone
θ_{M}	ratio of concentrations of inner-sphere complexes and reactive sites

References

(1) Buffle, J. *Complexation Reactions in Aquatic Systems: an Analytical Approach*; Ellis Horwood: Chichester, 1988.

(2) Duval, J. F. L.; Wilkinson, K. J.; van Leeuwen, H. P.; Buffle, J. Humic Substances are Soft and Permeable: Evidence from their Electrophoretic Mobilities. *Environ. Sci. Technol.* **2005**, *39*, 6435-6445.

(3) Chen, Z.; Campbell, P. G. C.; Fortin, C. Silver Binding by Humic Acid as Determined by Equilibrium Ion-Exchange and Eialysis. *J. Phys. Chem. A* **116**, 6532-6539.

(4) Buffle, J.; Zhang, Z.; Startchev, K. Metal Flux and Dynamic Speciation at (Bio)Interfaces. Part I: Critical Evaluation and Compilation of Physicochemical Parameters for Complexes with Simple Ligands and Fulvic/Humic Substances. *Environ. Sci. Technol.* **2007**, *41*, 7609-7620.

(5) Town, R. M.; Duval, J. F. L.; Buffle, J.; van Leeuwen, H. P. Chemodynamics of Metal Complexation by Natural Soft Colloids: Cu(II) Binding by Humic Acid. *J. Phys. Chem. A* **2012**, *116*, 6489-6496.

(6) Town, R. M.; van Leeuwen, H. P. Intraparticulate Speciation Analysis of Soft Nanoparticulate Metal Complexes. The Impact of Electric Condensation on the Binding of Cd^{2+}/Pb^{2+}/Cu^{2+} by Humic Acids. *Phys. Chem. Chem. Phys.* **2016**, *18*, 10049-10058.

(7) Town, R. M.; van Leeuwen, H. P. Dynamic Speciation Analysis of Heterogeneous Metal Complexes with Natural Ligands by Stripping Chronopotentiometry at Scanned Deposition Potential (SSCP). *Aust. J. Chem.* **2004**, *57*, 983-992.

(8) van Leeuwen, H. P.; Town, R. M. Electric Condensation of Divalent Counterions by Humic Acid Nanoparticles. *Environ. Chem.* **2016**, *13*, 76-83.

(9) Town, R. M.; van Leeuwen, H. P. Metal Ion – Humic Acid Nanoparticle Interactions: Role of Both Complexation and Condensation Mechanisms. *Phys. Chem. Chem. Phys.* **2016**, *18*, 18024-18032.

(10) Krishnan, K.; Plane, R. A. Raman Spectra of Ethylenediaminetetraacetic Acid and its Metal Complexes. *J. Am. Chem. Soc.* **1968**, *90*, 3195-3200.

(11) Clapp, L. A.; Siddons, C. J.; Whitehead, J. R.; van Derveer, D. G.; Rogers, R. D.; Griffin, S. T.; Jones, S. B.; Hancock, R. D. Factors Controlling Metal-Ion Selectivity in the Binding Sites of Calcium-Binding Proteins. The Metal-Binding Properties of Amide Donors. A Crystallographic and Thermodynamic Study. *Inorg. Chem.* **2005**, *44*, 8495-8502.

(12) Manning, G. S. Limiting Laws and Counterion Condensation in Polyelectrolyte Solutions. IV. The Approach to the Limit and the Extraordinary Stability of the Charge Fraction. *Biophys. Chem.* **1977**, *7*, 95-102.

(13) van Leeuwen, H. P.; Cleven, R. F. M. J.; Valenta, P. Conductometric Analysis of Polyelectrolytes in Solution. *Pure Appl. Chem.* **1991**, *63*, 1251-1268.

(14) Garcia-Fernandez, E.; Paulo, P. M. R.; Costa, S. M. B. Evaluation of Electrostatic Binding of PAMAM Dendrimers and Charged Phthalocyanines by Fluroescence Correlation Spectroscopy. *Phys. Chem. Phys.* **2015**, *17*, 4319-4327.

(15) Majtyka, M.; Klos, J. Monte Carlo Simulations of a Charged Dendrimer with Explicit Counterions and Salt Ions. *Phys. Chem. Chem. Phys.* **2007**, *9*, 2284-2292.

(16) Huang, Q. R.; Dubin, P. L.; Moorefield, C. N.; Newkome, G. R. Counterion Binding on Charged Spheres: Effect of pH and Ionic Strength on the Mobility of Carboxyl-Terminated Dendrimers. *J. Phys. Chem. B* **2000**, *104*, 898-904.

(17) Li, Z.; van Dyk, A. K.; Fitzwater, S. J.; Fichthorn, K. A.; Milner, S. T. Atomistic Molecular Dynamic Simulations of Charged Latex Particle Surfaces in Aqueous Solution. *Langmuir* **2016**, *32*, 428-441.

(18) Tipping, E. Humic Ion-Binding Model VI: An Improved Description of the Interactions of Protons and Metal Ions with Humic Substances. *Aquat. Geochem.* **1998**, *4*, 3-48.

(19) Warwick, P.; Hall, A.; King, S. J.; Zhu, J; van der Lee, J. Thermodynamic Aspects of Nickel Humic Acid Interactions. *Radiochim. Acta* **1998**, *81*, 215-221.

(20) Robertson, A. P.; Leckie, J. O. Acid/Base, Copper Binding, and Cu^{2+}/H^{+} Exchange Properties of a Soil Humic Acid, an Experimental and Modeling Study. *Environ. Sci. Technol.* **1999**, *33*, 786-795.

(21) Marsac, R.; Davranche, M.; Gruau, G.; Bouhnik-Le Coz, M.; Dia, A. An Improved Description of the Interactions Between Rare Earth Elements and Humic Acids by Modeling: PHREEQC-Model VI Coupling. *Geochim. Cosmochim. Acta* **2011**, *75*, 5625-5637.

(22) Bryan, N. D.; Jones, D. M.; Appleton, M.; Livens, F. R.; Jones, M. N.; Warwick, P.; King, S.; Hall, A. A Physicochemical Model of Metal-Humate Interactions. *Phys. Chem. Chem. Phys.* **2000**, *2*, 1291-1300.

(23) Duval, J. F. L. Electrokinetics of Diffuse Doft Interfaces. 2. Analysis Based on the Nonlinear Poisson-Boltzmann Equation. *Langmuir* **2005**, *21*, 3247-3258.

(24) Colla, T.; Likos, C. N.; Levin, Y. Equilibrium Properties of Charged Microgels: a Poisson-Boltzmann-Flory Approach. *J. Chem. Phys.* **141**, 234902.

(25) Duval, J. F. L.; van Leeuwen, H. P. Rates of Ionic Reactions with Charged Nanoparticles in Aqueous Media. *J. Phys. Chem. A.* **2012**, *116*, 6443-6451.

(26) Ohshima, H.; Kondo, T. Relationship Among the Surface Potential, Donnan Potential and Charge Density of Ion-Penetrable membranes. *Biophys. Chem.* **1990**, *38*, 117-122.

(27) Yezek, L. P.; van Leeuwen, H. P. Donnan Effects in the Steady-State Diffusion of Metal Ions through Charged Thin Films. *Langmuir* **2005**, *21*, 10342-10347.

(28) Levin, Y. Electrostatic Correlations: from Plasma to Biology. *Rep. Prog. Phys* **2002**, *65*, 1577-1632.

(29) Manning, G. S. The Molecular Theory of pPlyelectrolyte Solutions with Applications to the Electrostatic Properties of Polynucleotides. *Q. Rev. Biophys.* **1978**, *2*, 179-246.

(30) van Leeuwen, H. P.; Buffle, J. Chemodynamics of Aquatic Metal Complexes: From Small Ligands to Colloids. *Environ. Sci. Technol.* **2009**, *43*, 7175-7183.

(31) Filella, M.; Buffle, J.; van Leeuwen, H. P. Effect of Physico-Chemical Heterogeneity of Natural Complexants. Part I. Voltammetry of Labile Metal-Fulvic Complexes. *Anal. Chim. Acta* **1990**, *232*, 209-223.

(32) Buffle, J.; Altmann, R. S.; Filella, M.; Tessier, A. Complexation by Natural Heterogeneous Compounds: Site Occupation Distribution Functions, a Normalized Description of Metal Complexation. *Geochim. Cosmochim. Acta* **1990**, *54*, 1535-1553.

(33) van Leeuwen, H. P.; Buffle, J. Voltammetry of Heterogeneous Metal Complex Systems. Theoretical Analysis of the Effects of Association/Dissociation Kinetics and the Ensuing Lability Criteria. *J. Electroanal. Chem.* **1990**, *296*, 359-370.

(34) Soares, H. M. V. M.; Conde, P. C. F. L.; Almeida, A. A. N.; Vasconcelos, M. T. S. D. Evaluation of *n*-Substituted Aminosulfonic Acid pH Buffers with a Morpholinic Ring for Cadmium and Lead Speciation Studies by Electroanalytical Techniques. *Anal. Chim. Acta* **1999**, *394*, 325-335.

(35) Mash, H. E.; Chen, Y. -P.; Sigg, L.; Hari, R.; Xue, H. -B. Complexation of Copper by Zwitterionic Aminosulfonic (Good) Buffers. *Anal. Chem.* **2003**, *75*, 671-677.

(36) Vermeer, R. *Interactions Between Humic Acid and Hematite and Their Effects on Metal Ion Speciation*; PhD Thesis, Wageningen Agricultural University, 1996.

(37) Tan, W. F.; Koopal, L. K.; Norde, W. Interaction Between Humic Acid and Lysozyme, Studied by Dynamic Light Scattering and Isothermal Titration Calorimetry. *Environ. Sci. Technol.* **2009**, *43*, 591-596.

(38) Puy, J.; Galceran, J.; Huidobro, C.; Companys, E.; Samper, N.; Garcés, J. L.; Mas, F. Conditional Affinity Spectra of Pb^{2+}-Humic Acid Complexation from Data Obtained with AGNES. *Environ. Sci. Technol.* **2008**, *42*, 9289-9295.

(39) Abate, G.; Masini, J. C. Complexation of Cd(II) and Pb(II) with Humic Acids Studied by Anodic Stripping Voltammetry using Differential Equilibrium Functions and Discrete Site Models. *Org. Geochem.* **2002**, *33*, 1171-1182.

(40) Avena, M. J.; Koopal, L. K.; van Riemsdijk, W. H. Proton Binding to Humic Acids: Electrostatic and Intrinsic Interactions. *J. Coll. Interf. Sci.* **1999**, *217*, 37-48.

(41) Town, R. M.; van Leeuwen, H. P. Depletive Stripping Chronopotentiometry: a Major Step Forward in Electrochemical Stripping Techniques for Metal Ion Speciation Analysis. *Electroanal.* **2004**, *16*, 458-471.

(42) Galceran, J.; Companys, E.; Puy, J.; Cecília, J.; Garcés, J. L. AGNES: a New Electroanalytical Technique for Measuring Free Metal Ion Concentration. *J. Electroanal. Chem.* **2004**, *566*, 95-109.

(43) van Leeuwen, H. P.; Town, R. M. Electrochemical Metal Speciation Analysis of Chemically Heterogeneous Samples: the Outstanding Features of Stripping Chronopotentiometry at Scanned Deposition Potential. *Environ. Sci. Technol.* **2003**, *37*, 3945-3952.

(44) Town, R. M.; van Leeuwen, H. P. Depletive Stripping Chronopotentiometry: a Major Step Forward in Electrochemical Stripping Techniques for Metal Ion Speciation Analysis. *Electroanal.* **2004**, *16*, 458-471.

(45) van Leeuwen, H. P.; Town, R. M. Stripping Chronopotentiometry at Scanned Deposition Potential (SSCP). Part 3. Irreversible Electrode Reactions. *J. Electroanal. Chem.* **2003**, *556*, 93-102.

(46) Oldham, K. B.; Parry, E. P. Use of Polarography and Pulse-Polarography in the Determination of the Kinetic Parameters of Totally Irreversible Electroreductions. *Anal. Chem.* **1968**, *40*, 65-69.

(47) Town, R. M.; van Leeuwen, H. P. Fundamental Features of Metal Ion Determination by Stripping Chronopotentiometry. *J. Electroanal. Chem.* **2001**, *509*, 58-65.

(48) von Wandruszka, R. The Micellar Model of Humic Acid: Evidence from Pyrene Fluorescence Measurements. *Soil Sci.* **1998**, *163*, 921-930.

(49) van der Wal, A.; Minor, M.; Norde, W.; Zehnder, A. J. B.; Lyklema, J. Electrokinetic Potential of Bacterial Cells. *Langmuir* **1997**, *13*, 165-171.

(50) Ohshima, H.; Ohki, S. Donnan Potential and Surface Potential of a Charged Membrane. *Biophys. J.* **1985**, *47*, 673-678.

(51) Millero, F. J.; Gombar, F.; Oster, J. The Partial Molal Volume and Compressibility Change for the Formation of the Calcium Sulfate Ion Pair at 25°C. *J. Sol. Chem.* **1977**, *6*, 269-280.

(52) Hamm, L. M.; Wallace, A. F.; Dove, P. M. Molecular Dynamics of Ion Hydration in the Presence of Small Carboxylated Molecules and Implications for Calcification. *J. Phys. Chem. B* **2010**, *114*, 10488-10495.

Table of contents graphic

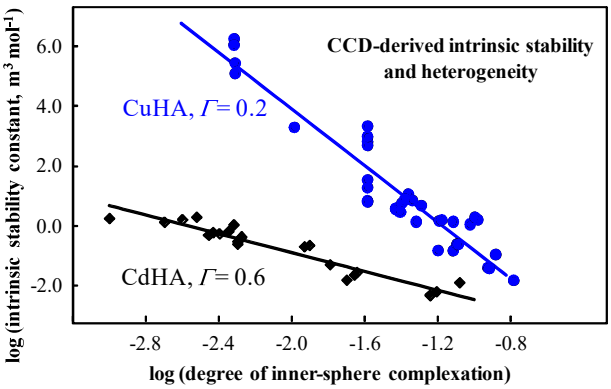
CCD-derived intrinsic stability
and heterogeneity
CuHA, Γ= 0.2
CdHA, Γ= 0.6
log (intrinsic stability constant, m3 mol-1)
log (degree of inner-sphere complexation)
6.0
4.0
2.0
0.0
-2.0
-2.8
-2.4
-2.0
-1.6
-1.2
-0.8